CFD Letters

Journal homepage:
https://semarakilmu.com.my/journals/index.php/CFD_Letters/index
ISSN: 2180-1363

Numerical Model Parameters Impact on Savonius Wind Rotor Performance

Mariem Lajnef[1], Mabrouk Mosbahi[2,3,*], Zied Driss[1], Emanuele Amato[3,4], Tullio Tucciarelli[3,4], Marco Sinagra[4], Calogero Picone[4]

[1] Laboratory of Electro-Mechanic Systems (LASEM), National School of Engineers of Sfax (ENIS), University of Sfax, B.P. 1173, km 3.5 Soukra, 3038 Sfax, Tunisia
[2] University of Tunis, Higher National Engineering School of Tunis (ENSIT), Avenue Taha Hussein Montfleury, 1008, Tunisia
[3] University of Palermo, Department of Engineering, 90128, Italy
[4] Sustainable Mobility center (Centro Nazionale per la Mobilita Sostenible-CNMS), Italy

ARTICLE INFO

Article history:
Received 23 January 2024
Received in revised form 18 March 2024
Accepted 8 April 2024
Available online 30 November 2024

Keywords:
Savonius wind rotor; numerical model; validation; torque coefficient; power coefficient

ABSTRACT

Global greenhouse gas emissions are mostly caused by the production of energy extracted from fossil fuels sources. Indeed, the use of renewable clean energy has become crucial to supply the world demand while protecting the planet. For many years, there has been a great deal of interest in wind energy because it is a clean, sustainable energy source. Because of its cheaper cost and independence from wind direction, the Savonius vertical axis wind rotor has the advantage of being suitable for certain implementations as an energy converter. Several studies have been carried out to increase its efficiency from this angle. This research work emphasizes on the Savonius wind rotor numerical model performances. The main goal is to explore the impact of setting the numerical model parameters on its aerodynamic and performance characteristics. Ansys Fluent software 17.0 was utilized to perform numerical simulations utilizing the unsteady Reynolds-Averaged Navier-Stokes (URANS) equations. The mesh sizing, the turbulence model as well as the time step parameters were investigated. The numerical model validation was realized through published experimental findings available in the literature for an inlet wind velocity of 6 ms^{-1}. Good accordance was obtained. Thus the numerical model with the selected parameters was relevant for further investigations. For a tip speed ratio λ=0.64 it gave a torque and power coefficients equal to 0.328 and 0.2, respectively.

1. Introduction

Energy production is responsible for most of the greenhouse gas emissions globally. Without changes to the energy production strategy, climate change will continue to cause irrecoverable changes to the environment. Hence, it became crucial to switch to renewable energy sources. They provides reliable power supplies and fuel diversification, which enhance energy security, lower risk of fuel spills, and reduce the need for imported fuels. It also helps conserve the nation natural resources. Its major sources are biomass, hydropower, geothermal, wind and solar. Wind energy in

* *Corresponding author.*
E-mail address: mabrouk.mosbahi@gmail.com (Mabrouk Mosbahi)

https://doi.org/10.37934/cfdl.17.5.5875

particular offers many advantages, which explains why it is one of the fastest-growing energy sources in the world. For as long as the sun shines and the wind blows, the energy produced can be harnessed to send power across the grid. Thus, it is a sustainable form of energy. In order to convert wind energy into electricity, investors mostly invest in large wind turbine farms which are basically a group of wind turbines in the same location used to produce electricity on a large scale [1]. However, investing in small scale turbines became tempting nowadays as more and more individuals are aware of the importance of clean energy [2, 3].

Wind turbines are designed according to different geometries [4] and classified based on the axis rotation, into horizontal axis wind turbine (HAWT) and vertical axis wind turbine (VAWT).The particularity of VAWT is its ability to function regardless to the wind direction and is less likely to be affected by the extremely strong wind stream. Another major advantage is that its acoustics are less disturbing and being a small-scaled design, it is much easier to be integrated into buildings. Nevertheless, VAWTs are not as popular as HAWTs. Because of their relatively small size, the produced energy is low [5] and do not encourage investment. However, they are adaptive to energy needs of consumers of houses and apartments. VAWT are divided into two categories, the drag-based devices that use aerodynamic drag to extract power from the wind, and the lift-based types. Two models were in the stage of commercialization, which are Savonius rotor and Darrieus rotors.

Regarding the Savonius wind turbine, it consists of two blades with a design of a half a circle arranged in the shape of S. The wind blows its way through these blades, causing the axis to spin to generate electricity. Technically speaking, its principle is based on an aerodynamic torque induced by the air flow in the structure created by Savonius. This turbine exhibits numerous advantages like its decent efficiency and its low noise level. Also despite the Darrieus wind rotor, the Savonius wind rotor is self-starter. Despite their qualities, Savonius type wind turbines have weak points. First of all, the significant mass of the rotor is the cause of efficiency reduction due to the induced inertia. Also, the bucket offering its convex face to the wind is not, by definition, as efficient as one which at the same time offers its concave face to the wind blows which results in a resistive torque. But when the cost and above all the reliability of the installation outweigh the efficiency, then it is still a good choice. Based on the review of literature, there has been a great deal of interest in the conventional Savonius wind turbine. In fact, a lot of study has been done to increase its efficiency by optimizing its geometrical parameters.

The number of research works examining computational methods has increased in the last several years. Ebrahimpour *et al.,* [6] carried on the effect of the overlapping technique. The investigation was conducted with a numerical approach. Different overlap ratios were investigated ranged from -0.4 to 0.4 to obtain the optimum value. In order to mesh the numerical model, a sliding mesh method was used. After testing different mesh sizes in order to obtain the most relevant one, the simulations performed with Ansys fluent generated the torque and the power coefficients for each tested overlap. The optimal result was the ratio of 0.15 for which the power coefficient was almost equal to C_P= 20%. Sobczak *et al.,* [7] investigated the aspect ratio impact. The tested aspect ratios ranged from 0.5 to 5. The effect of the aspect ratio was tested initially on the same tip speed ratio λ=0.8. Then the power coefficient was analyzed for aspect ratios equal to 0.5, 1.5 and 5. The maximum power coefficients were equal to 21.8 %, 20.6 % and 17.7 %, respectively, for 5, 1.5 and 0.5 aspect ratios. Thus, the aspect ratio of 5 was found the optimum one with improved performances. Lee *et al.,* [8] explore the effect of the twist angle parameter using both an experimental and numerical method on a conventional Savonius wind rotor. Four different angles were tested which are 0°, 45°, 90° and 135°. Both approaches were used in order to compare the results and better evaluate the performance of the rotor. It was noted that the peak

of the power coefficient was between λ=0.5 and λ=0.65 for all twist angles. The performance of the Savonius wind turbine was noted to be the most efficient for a twist angle equal to 45° from both the experiments and numerical analysis, with a power coefficient equal to C_P=0.13 at λ= 0.54. Whereas, the 135° twist angle gave the lowest power coefficient of C_P=0.12 at λ=0.54. In the same vein, , in comparison to a simple Savonius wind turbine, twisted Savonius wind turbine with a conical shaft showed better performances with an 18% increase in the power coefficient, a 31% increase in the discharge flow rate and lesser negative torque according to Tahani *et al.,* [9]. Tian *et al.,* [10] investigated numerically the blade shape effect. More specifically, they tested the effect of the inner blade position throughout the software Ansys Fluent. Five values of the inner blade position were simulated which are 100°, 120°, 140°, 160° and 180°.The inner blade angle is the angle that corresponds to the inner blade opening, for instance, a conventional Savonius wind turbine inner blade angle was equal to 180°. The maximum power coefficient was obtained with the angle of 120° and it is equal to C_P= 19%. The least performant angle is 180° where the peak of the power coefficient was equal to C_P=15.5%. In the same context, a CFD investigation was carried out by Syahreen *et al.,* [11] to assess the performance of a Savonius wind turbine with a novel blade shape design. The wind speed impact was studied. An improvement of 20 % was recorded with the novel design over the classical elliptical Savonius wind rotor. The blade arc angle was also investigated .In this context, Akhlaghi *et al.,* [12] tested through three dimensional simulations three different arc blade. Results indicated that the highest power coefficient of 0.0261 and torque coefficient of 0.501 were obtained at an arc angle of 180°. Besides, a new model of Savonius wind turbine was numerically examined by Sohib *et al.,* [13] through the addition of tubercles at the level of the rotor blades. With an improvement of up to 46.15 %, the new turbine model fitted with tubercles outperformed the baseline model. The flow visualizations revealed decreased wake diameters, which indicate less drag and ultimately results in a better performance when compared to the baseline model. The end plates addition to the conventional Savonius wind rotor components has demonstrated an improvement in its efficiency. The use of end plates prevents the escape of the air from the concave sides of both blades. It forces the air to leave the concave advancing blade to the concave returning blade. Indeed, it keeps the pressure difference between the concave and the convex side of the rotor blades higher over the rotor height. Subsequently, it reduces the negative drug and enhances the process of energy conversion. In this regard, Jeon *et al.,* [14] investigated numerically the effect of end plates on the torque and power coefficient of a 180° twisted Savonius rotor. The studied rotors were taken, respectively, without end plates, with only lower end plate and with both upper and lower end plates. To show the effect of the end plate size and shape, they varied the ratio between the end plate area to the cross sectional area. The end plates size affects the maximum output power coefficient which increases with the rise of end plate size. Thus, the upper and lower end plates with circular shape are found the optimum design that improves the efficiency of the studied helical Savonius rotor by 36% at a wind velocity of 10 $m.s^{-1}$ over the non-end plates design. Zheng *et al.,* [15] carried out a numerical study for modified Savonius rotor with four, five and six blades. They found that the maximum power coefficient was equal to 27.14%, 28.493% and 30.564% at a rotating speed equal to Ω=17.206, Ω=16.265 and Ω=18.369 rpm, respectively for four, five and six bladed rotors. The efficiency of the modified Savonius rotor increases with the increase of the blades number. Thus, the six-bladed design was found the optimum. This fact was also found numerically with Emmanuel *et al.,* [16]. Mohamed *et al.,* [17] employed an obstacle plate to partially cover the Savonius wind rotor returning blade on models with two and three blades. They discovered that the barrier for its various configurations enhanced the self-starting capabilities based on CFD simulations. In fact, it led to a positive static moment at all angular positions. For both the two and three bladed rotors, the shielding obstacle

position was tuned to raise the maximum power coefficient by 27.5% and 27.3%, respectively. In the same context, the numerical research of Payambarpour *et al.,* [18] examined a two-bladed Savonius rotor with an upstream-mounted deflector. Across pressure contours and 3D streamlines, the effects of changing the suggested deflector and the rotor geometrical characteristics on the flow rate, output torque, and rotor efficiency were discussed. An increase in turbine height was shown to have a positive impact. The outcomes demonstrated that raising the turbine height had a positive impact. Nevertheless, the performance of the turbine was negatively impacted by raising the deflector parameters above a specific threshold. Farajyar *et al.,* [19] carried out a CFD simulation on the impact of different operating parameters. After finding the optimized design, they demonstrated that by diverting airflow, putting in a curtain in the rotor upstream part increases the power coefficient value. Furthermore, the generated power increased with an increase in the inlet wind velocity subsequently the Reynolds number.

As was already noted, researchers examined the performance of the VAWT using computational techniques. Upon reviewing the literature on the Savonius wind rotor, it is evident that there is a dearth of research focusing mainly on the impact of selecting numerical model parameters on the rotor performance. In this context, the majority of research was done to optimize geometrical parameters in order to enhance its performance. Selecting the numerical model parameters is a necessary yet delicate undertaking. Regarding this research work, the basic objective is to investigate the numerical model parameters effect on the performance of a conventional Savonius wind rotor namely the meshing size, the turbulence model and the time step size. Experimental findings taken from a previously published study served as the basis for selecting the appropriate parameters and validating the numerical model. The numerical study was realized through 3D (three dimensional) transient simulations investing the CFD Ansys Fluent 17.0 software.

2. Physical Model

The aim of the numerical investigation is to obtain results and compare them to the experimental one of realized by Roy *et al.,* [20]. For that purpose, the numerical model should be valid and appropriate. For that, the numerical model as shown in Figure 1 concerns a conventional Savonius wind rotor that was used by Roy *et al.,* It consists of two semi cylindrical blades offset from each other by an overlap distance and limited on the top and the bottom by two end plates. Table 1 shows the general geometrical parameters.

Table 1
Geometrical parameters of the studied Savonius wind rotor

Parameter	Value
Overall diameter, D	210 mm
Rotor height, H	230 mm
End plate diameter, D_e	230 mm
Blade chord, d	117 mm
Blade thickness	0.63 mm
Overlap distance, e	23.4 mm

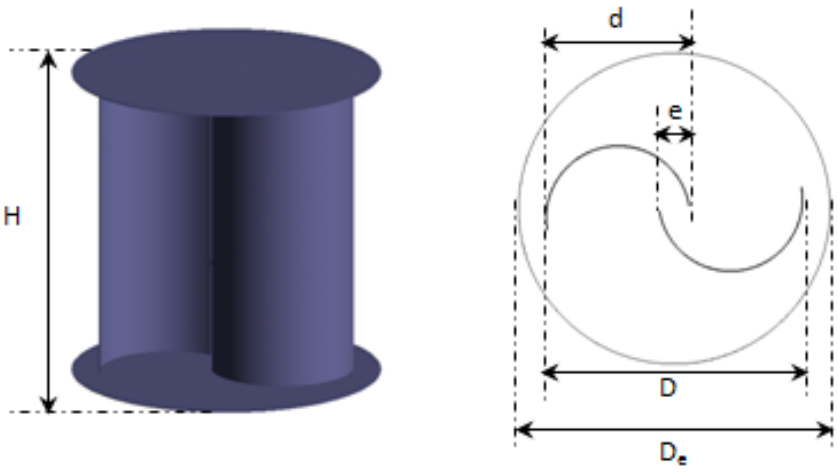

(a) (b)

Fig. 1. Savonius rotor numerical model (a) Isometric view (b) Sectional view

3. Numerical Methodology

Fluid mechanics is the study of liquids and gases at two states, which are stationary state and dynamic state. In fact, fluid dynamic, which is the study of fluid in motion, describes how the flow is altered by outer forces and interactions with boundaries. Computational fluid dynamics is the process of mathematically modeling those physical phenomena implying fluid flow and solving it numerically using computational process. CFD is useful in wide variety of applications [21-27]. An aerodynamic study is crucial when optimizing a design. Usually, the only way to proceed is through conducting physical tests on product prototypes. With the prosperity of computational power, the field of computational fluid dynamics became a commonly applied tool for generating solutions and results. Basically, the strategy of the CFD is to replace the continuous problem domain with a discrete domain. The cornerstone of this study is the fundamental governing equations of fluid dynamics; the continuity and the momentum. These equations are known as the Navier-Stokes equations [28-30]. Thanks to CFD, the Navier-Stokes would be solved in a discrete domain. Three-dimensional transient simulations using ANSYS FLUENT 17.0 were carried out for the current investigation. The modeling of wind flow surrounding the analyzed rotor depends on solving the Navier-Stokes equations that govern it.

3.1 Computational Domain and Boundary Conditions

The computational domain was created using ANSYS Design Modeler, and as shown in Figure 2, the required boundary conditions were found. The computational domain is divided into two domains which are the rotating and the stationary domain that represents the wind tunnel test chamber used in the experiments of Roy *et al.,* [20]. These two domains are separated by a sliding surface. The stationary domain has the following dimensions: 500 mm ×500 mm × 700 mm. The rotational domain has a cylindrical shape. It contains the Savonius wind rotor and rotates with the same rotational speed of Ω= 32.82 rad/s. The surfaces of the Savonius rotor are considered as walls. A velocity of V= 6 m/s is defined as an inlet boundary condition and it is located at 250 mm from the rotor rotation axis. An atmospheric pressure is defined as an outlet boundary condition and it is located at 450 mm from rotor rotation axis. Boundary walls are set for the rest of the test chamber sides with a symmetry condition.

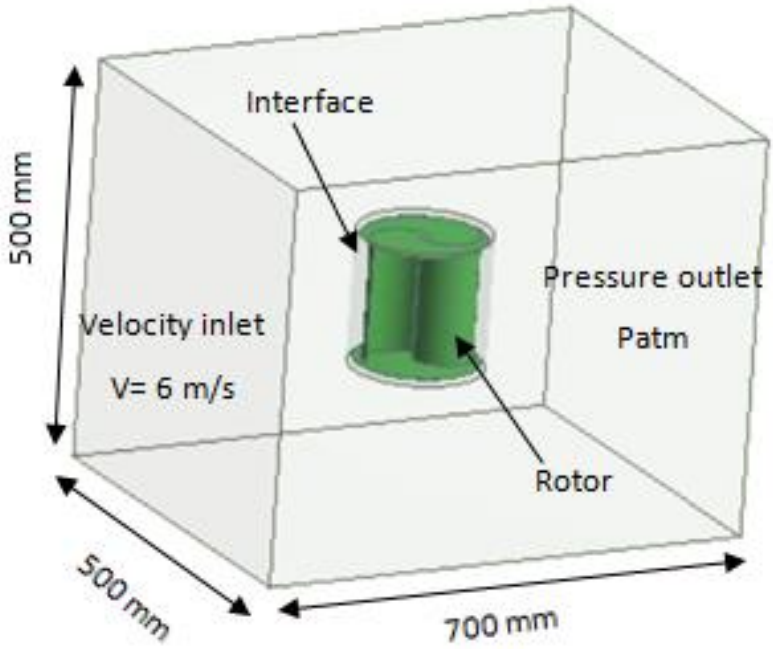

Fig. 2. Computational domain and boundary conditions

3.2 Meshing

Ansys provides general purpose, high-performance, automated, intelligent meshing software that produces the most appropriate mesh for accurate and efficient multiphysics solutions, from easy, automatic meshing to highly crafted mesh. Smart defaults are built into the software to make meshing a painless and intuitive task, delivering the required resolution to capture solution gradients properly for dependable results. The meshing of the considered model is triangular. In order to refine the mesh, each domain elements size was controlled through the sizing feature in Ansys meshing. When getting closer to the rotor blades, the size of elements decreases. To do so further and to capture the rapid variations of the aerodynamic characteristics around the studied rotor, it was recommended to create inflation near the rotor walls sufficiently. Thus, 20 prismatic layers were created at the level of boundary layers and especially at the rotor blades.

The suitability of the generated mesh depends on the choice of the distance of the first mesh node from the rotor walls (y_n). y^+ is the appropriate parameter to estimate y_n based on Eq. (1). The accurate value of y^+ depends on the turbulence model walls law. As the SST k-ω model was used under this study, an y^+ almost equal to 1 was associated.

$$y^+ = \frac{\rho u_t y_n}{\mu} \tag{1}$$

Where ρ is the air density (kg.m^{-3}), u_t is the friction velocity (m.s^{-1}) and μ is the viscosity of the fluid (Pa.s).

As the mesh is one of the most important influences in CFD simulation, the meshing size effect was investigated. So, six different meshes with multiple element size as presented in Figure 3 were tested to investigate the effect of the mesh sizing on the performance of the studied Savonius wind rotor and to justify the chosen value. All mesh details are presented in Table 2.

Table 2
Mesh sizing properties

Case	1	2	3	4	5	6
Number of elements	678487	937765	1221196	1988771	2006180	2498249
Number of nodes	127230	171509	226154	357977	368501	455899
Element size of stationary domain (m)	0.02	0.021	0.0161	0.016	0.014	0.012
Element size of rotating domain (m)	0.01	0.01	0.0091	0.009	0.0071	0.007
Element size on blade (m)	0.006	0.0055	0.0045	0.004	0.0035	0.003
Y+	1	1	1	1	1	1
Number of boundary layers	20	20	20	20	20	20
Skewness	0.89	0.88	0.87	0.85	0.84	0.84

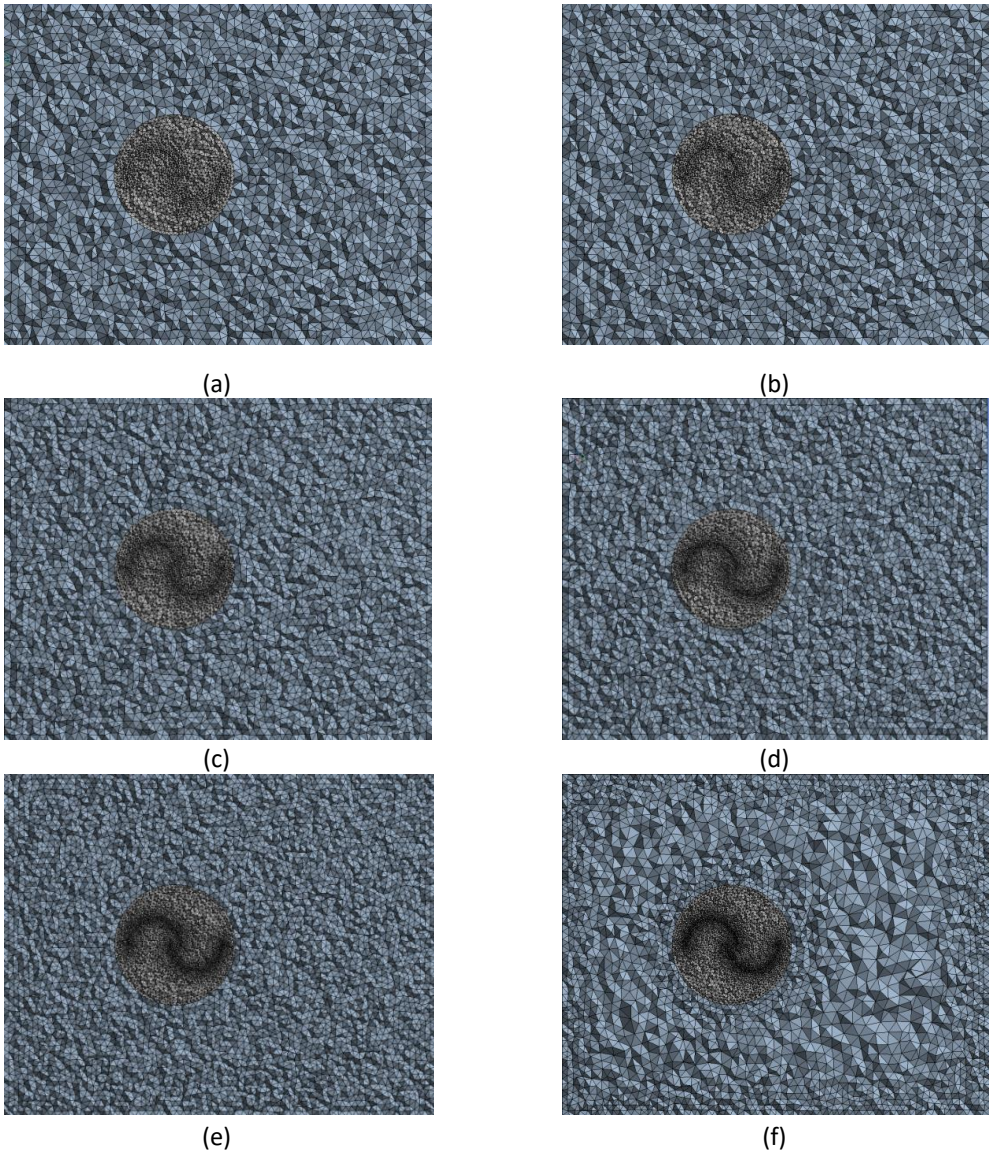

Fig. 3. Tested meshes (a) Case 1 (b) Case2 (c) Case 3 (d) Case 4 (e) Case 5 (f) Case 6

3.3 Numerical Settings

The flow around the studied Savonius wind rotor is naturally turbulent. For that, 3-D transient simulations were run. The resolution process is basically assigning a number of full rotations for the rotor to achieve, and in each single round the values of moment coefficient would be saved from

predefined angular positions. In this numerical model, the rotation of the turbine was chosen through an angle of θ= 10°. As a result, the size of the time step (Δt) was determined using the following formulation:

$$\Delta t = \frac{\Delta\theta}{\Omega} \tag{2}$$

Where $\Delta\theta$ is the rotor rotation angle (rad) and Ω sets for the rotor rotation speed (rad/s).

A time step study was carried out to show the effect of this parameter on the performance of the studied Savonius wind rotor and to justify the chosen value. In order to obtain accurate results, the rotor would perform minimum four rotations. So the number of time steps was set equal to N=144 and maximum iteration per time step was set equal to 70 iterations.

The required reference values need to be regulated such as the area, density, enthalpy, length, the velocity ect. The reference area was set as the swept area (A) defined based on Eq. (3). For the length, it was set as the rotor radius (R). The velocity was computed from the inlet which value was equal to V= 6 m/s and the air density value was equal to ρ=1.225 kg.m^{-3}. The other values were set by default.

$$A = DH \tag{3}$$

Where D and H are the diameter and the height of the rotor (m), respectively.

The residual is simply the error between the current and the previous output. The error is compared to the convergence criteria which was set equal to 10^{-6} and the solution is theoretically considered converged when the residuals go below the convergence criteria.

To proceed the simulation, a solution method had to be selected from 4 methods available which are SIMPLE, SIMPLEC, PISO and COUPLED. Each one is adequate for a specific application and circumstances. The COUPLED algorithm is often a must-use with transient flow. This algorithm enables full pressure-velocity coupling to induce a constraint on the solution. For more accuracy then, COUPLED solution method was chosen as a solution method.

Navier-Stokes equations govern the physics of fluid flow [31-33]. As they are arranged using a high order non-linear partial differential equations, they cannot be solved analytically. Therefore, a numerical method is needed. Finite Volume Method was used to discretize them. The convective terms as well as the temporal ones were discretized using the Second order Up-wind scheme. The Navier-Stokes governing equations according to a Newtonian fluid are prescribed under two equations: the continuity expressed in Eq. (4) and the momentum expressed in Eq. (5).

$$\frac{\partial\rho}{\partial t} + \frac{\partial\left(\rho u_i\right)}{\partial x_i} = 0 \tag{4}$$

Where t is the time (s) and u_i is the velocity component defined in the x_i coordinate direction x_i=(x,y,z).

$$\frac{\partial\left(\rho u_i\right)}{\partial t} + \frac{\partial\left(\rho u_i u_j\right)}{\partial x_j} = -\frac{\partial p}{\partial x_i} + \frac{\partial}{\partial x_j}\left[\mu\left(\frac{\partial u_j}{\partial x_j} + \frac{\partial u_j}{\partial x_i} - \frac{2}{3}\delta_{ij}\frac{\partial u_i}{\partial x_i}\right)\right] + \frac{\partial\left(-\rho\overline{u_i' u_j'}\right)}{\partial x_j} + F_i \tag{5}$$

Where p is the pressure (Pa) and F_i is the external forces applied (N).

The components of the Reynolds stress tensor are expressed mathematically through Eq. (5).

$$-\rho\overline{u_i' u_j'} = \mu_t\left(\frac{\partial u_i}{\partial x_j}+\frac{\partial u_j}{\partial x_i}\right)-\frac{2}{3}\rho k\delta_{ij} \tag{6}$$

Where μ_t is the turbulent viscosity (Pa.s), x_i, x_j are the Cartesian coordinate, k is the turbulent kinetic energy (Pa.s) and δ_{ij} is the Chronecker indices.

For the current simulations, the Shear Stress Transport SST k-ω model was chosen. Its strong modeling of wind turbines and superior flow pattern prediction have been shown by numerous researches [34, 35]. The SST k-ω model, in actuality, combines the freedom of the k-ε model in the far wall sections with the accuracy and robustness of the k-ω model in the near wall regions. It was specifically developed to calculations in near-wall region with the free-stream independence of the k-ε model in the far field. To achieve this, the k-ε turbulence model is converted in k-ω formulation.

The turbulence kinetic energy (k) is expressed as follows:

$$\frac{\partial(\rho k)}{\partial t}+\frac{\partial(\rho u_i k)}{\partial x_i}=\frac{\partial}{\partial x_i}\left[\left(\mu+\frac{\mu_t}{\sigma_k}\right)\mathrm{grad}(k)\right]+2\mu_t\frac{\partial u_i}{\partial x_j}\cdot\frac{\partial u_i}{\partial x_j}-\frac{2}{3}\rho k\frac{\partial u_i}{\partial x_j}\delta_{ijk}-\beta^*\rho k\omega \tag{7}$$

The specific dissipation rate (ω) is written as follow

$$\frac{\partial\rho\omega}{\partial t}+\frac{\partial(\rho u_i\omega)}{\partial x_i}= \\ \frac{\partial}{\partial x_i}\left[\left(\mu+\frac{\mu_t}{\sigma_{\omega,1}}\right)\mathrm{grad}(\omega)\right]+\gamma_2\left(2\rho\frac{\partial u_i}{\partial x_j}\cdot\frac{\partial u_i}{\partial x_j}-\frac{2}{3}\rho\omega\frac{\partial u_i}{\partial x_j}\delta_{ij}\right)-\beta_2\rho\omega^2+2\frac{\rho}{\sigma_{\omega,2}\omega}\frac{\partial k}{\partial x_k}\frac{\partial\omega}{\partial x_k} \tag{8}$$

Where μ is the dynamic viscosity (Pa.s) and β^*, β_2, σ_k, $\sigma_{\omega,1}$, $\sigma_{\omega,2}$ and γ_2 are the constants of the SST k-ω turbulence model.

Four turbulence models namely the standard k-ω, the SST k-ω, the BSL k-ω and the standard k-ε were putted to test under this study to show the effect of the turbulence model on aerodynamic and performance characteristics of the Savonius wind rotor and to justify the chosen value.

4. Numerical Model Choice and Validation

The torque coefficient of the studied Savonius wind rotor was chosen as an output parameter to show the effect of the considered parameters. It is considered stable with a periodic evolution when it oscillates around the same average value. Under the present study, the consistent state is obtained after four revolutions. It is defined based on Eq. (9)

$$C_m = \frac{T}{\frac{1}{2}\rho R A U_\infty^2} \quad (9)$$

Where T is the dynamic torque (N) and U_∞ is the incoming air velocity (m.s^{-1}).

4.1 Meshing Size Effect

In this section, as the mesh is one of the most important influences in CFD simulation, six different meshes as presented in Figure 3 with multiple element size as highlighted in Table 2 were putted to test to investigate the effect of the meshing size. Simulations were generated for λ= 0.64 corresponding to an angular velocity of Ω= 32.82 rad/s. The instantaneous output torque coefficients for all tested mesh were superposed and shown in Figure 4. According to these results, it is clear that the meshing size affects the variation of the numerical torque coefficient of the Savonius wind rotor. The gap between the different cases remains significant, especially for case 1 which corresponds to the coarse mesh. For other cases, the variation of the torque is close one from the other and persists very close for the refined meshes especially. Moreover, the average value ($Cm_{,num}$) as well as the computational time for the tested meshes are presented in Table 3 and compared to the experimental one ($Cm_{,exp}$) derived from the study of Roy *et al.,* [20] with the corresponding error value to assess the accuracy of each single mesh. For the coarse meshes, numerical torqueses are distant from the experimental one. The value of the error is equal to E= 16.9%. However, the computational time is remarkably brief. For the medium meshes like case 2, 3 and 4, a decrease in the value of the error to the proximity of E= 10% was noted. In these cases, the computation time varies depending on the used computer processor. As for the final mesh (case 6) which is the finest, the value of the torque coefficient is more accurate and the error value reached E=8.8%. A good agreement between numerical and experimental findings was recorded. Then the case 6 meshing with a global nodes number equal to 455899 was chosen for more precision and accuracy.

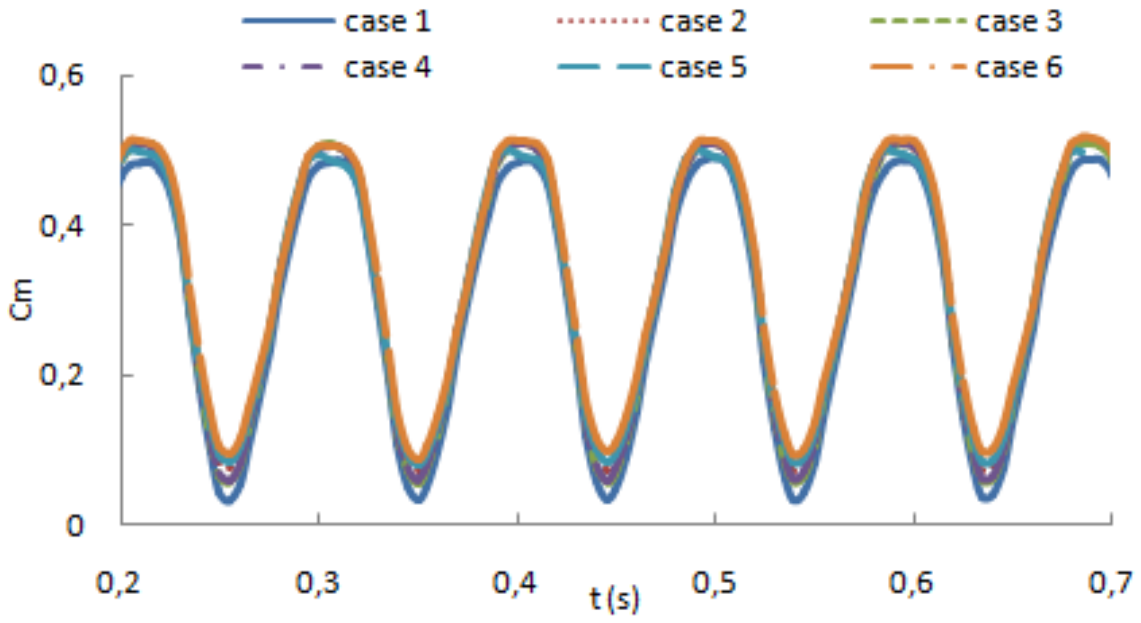

Fig. 4. Meshing size effect on the torque coefficient for λ= 0.64

Table 3
Comparison between numerical and experimental results for meshing effect

Case	Elements number	Nodes number	Cm_{num}	Cm_{exp}	Error	Calculation time	
						I7 computer	Station
1	678487	127230	0.299	0.36	16.9%	-	1 day
2	937765	171509	0.317	0.36	11.9%	2 days	-
3	1221196	226154	0.319	0.36	11.38%	-	2 days
4	1988771	357977	0.322	0.36	10.55%	3 days	-
5	2006180	368501	0.325	0.36	9.7%	-	5 days
6	2498249	455899	0.328	0.36	8.88%	6 days	-

4.2 Turbulence Model Effect

The aim of the performed simulations was to test the effect of the turbulence model. For that, four turbulence models were tested: the standard k-ω, the SST k-ω, the BSL k-ω and the standard k-ε. In fact, the chosen turbulent model affects the numerical model and the obtained results. Figure 5 presents the comparison of the instantaneous torque coefficient for the four tested turbulence models. The torque coefficient is clearly very near to the BSL k-ω and the SST k-ω and standard k-ω turbulence models. However, the standard k-ε is quite distant from them. Then the obtained results were compared with the experimental one and presented in Table 4 in order to evaluate one is closest to the flow reality and proves the agreement. The error was fond equal to 10.8% for the standard k-ω, 9.72% for the BSL k-ω, 8.33 % for the standard k-ε and 8.88 % for the SST k-ω turbulence model. So these last two models gave a good agreement with experimental findings. As the SST k-ω turbulence model is the most used in aerodynamics it was selected for more precision.

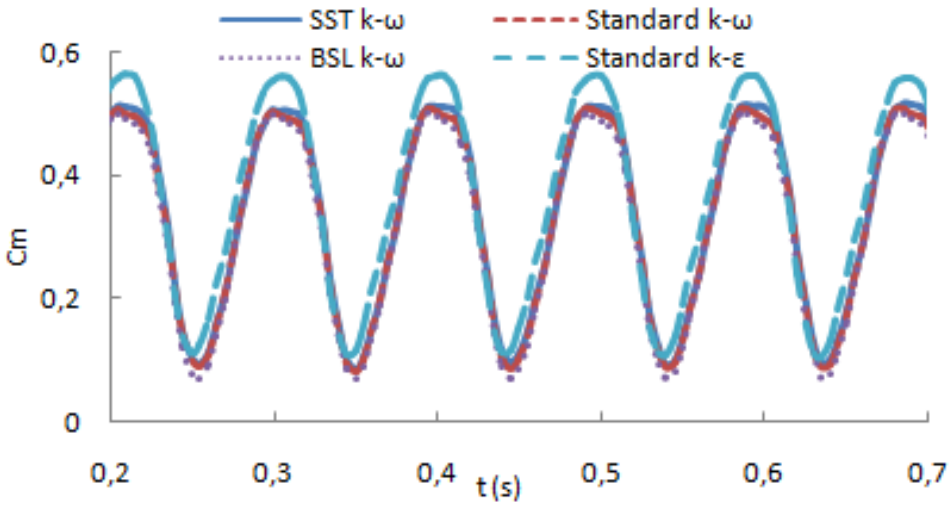

Fig. 5. Turbulence models effect on the torque coefficient for λ= 0.64

Table 4
Comparison between numerical and experimental results for turbulence model effect

Turbulence models	Cm_{num}	Cm_{exp}	Error
Standard k-ω	0.321	0.36	10.8%
SST k-ω	0.328	0.36	8.88%
BSL k-ω	0.325	0.36	9.72%
Standard k-ε	0.39	0.36	8.33%

4.3 Time Step Effect

Time step size is basically the discretization of the spatial grid in order to provide numerical results. The selection of the time step size affects the stability and the convergence of the solution. For that reason, choosing the appropriate value as well as the right number of time step setting is important to have accurate results. It is well known that Savonius rotor is unsteady by nature so a convenient time step size is required to incur large computational cost. For that, four different time step sizes were tested with values equal to t_{ss}=0.0052 s, t_{ss} =0.0104 s, t_{ss} =0.0156 s and t_{ss} =0.0208 s corresponding respectively to the rotation of the turbine through an angle of θ=10°, θ=20°, θ=30° and θ=40°. It is trivial that with small time step size the results would be more accurate however it would require long calculation time. Figure 6 presents a superposition of the instantaneous torque coefficient for the four tested time steps. It is clear that the choice of the time step affects the variation of the torque coefficient. The obtained results were compared with the experimental results and presented in Table 5 in order to evaluate which time step size is more accurate. For instance, the error increases with the increase in the angle of the turbine rotation. It is equal to 44.7%, 29.4%, 23.6% and 8.88 % respectively for θ=40°, θ=30°, θ=20°and θ=10°. Thus, the time step corresponding to θ=10° gave a numerical torque coefficient closer to the experimental one than the others. So good agreement was recorded with the minimize error.

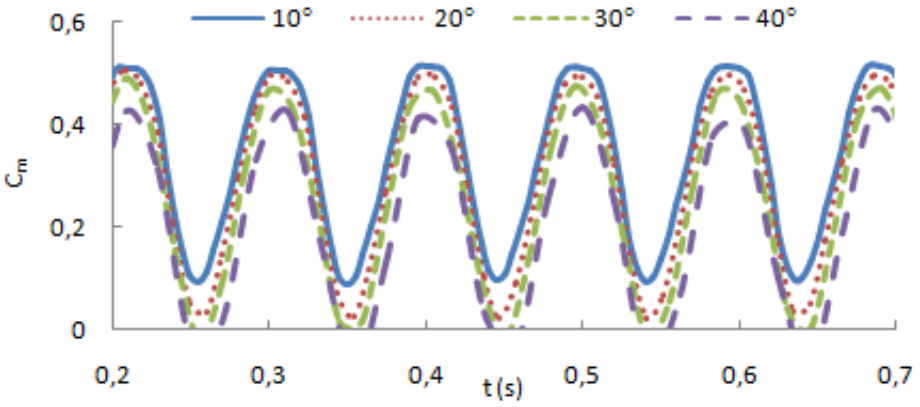

Fig. 6. Time step size effect on the torque coefficient for λ= 0.64

Table 5
Comparison between numerical and experimental results for time step effect

Turbine rotation angle	Time step size(s)	Cm_{exp}	Cm_{num}	Error (%)
10°	0.0052	0.36	0.328	8.88
20°	0.0104	0.36	0.275	23.6
30°	0.0156	0.36	0.254	29.4
40°	0.0208	0.36	0.199	44.7

A superposition of the numerical power coefficients derived from the adopt numerical model and the experimental ones taken from the experimental study of Roy *et al.,* [20] versus the tip speed ratios are presented in Figure 7. Under these conditions, the chosen numerical model derived from the mesh sizing, the turbulence model and the time step study was find with good agreement with the experimental findings of Roy *et al.,* [20] Then, it was validated with a average error equal to 8.8 %.

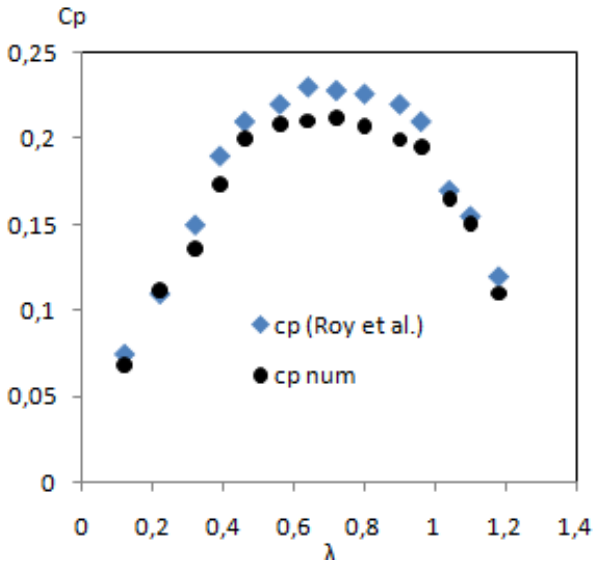

Fig. 7. Numerical model validation

5. Aerodynamic Characteristics

Two planes were selected to display the velocity fields, the total pressure, the turbulent kinetic energy and the viscosity distributions: a longitudinal plane defined by z=0 mm and a transverse plane defined by x=0mm. The two planes are presented in Figure 8.

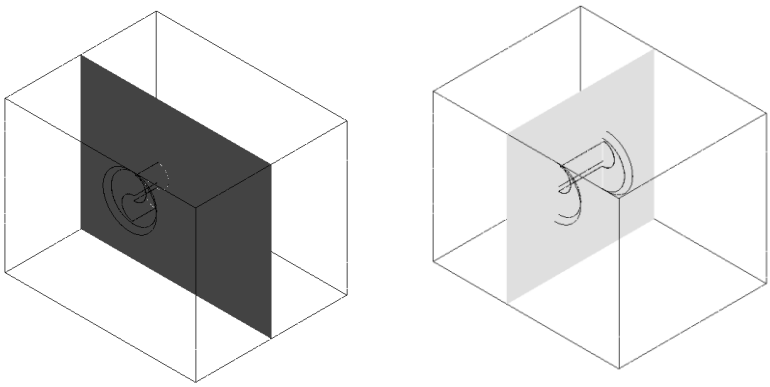

(a) (b)

Fig. 8. Presentation planes (a) z=0 mm (b) x=0 mm

5.1 Velocity Fields

Figure 9(a) and Figure 9(b) show the distribution of the velocity fields in the longitudinal plane defined by z=0 mm as well as the transverse plane defined by x=0 mm. From these results, the air stream is uniform at the inlet of the control volume with a velocity value equal to V= 6 m/s as set in the inlet boundary conditions. By approaching to the turbine, the velocity of the wind decreases. Near the blades, the velocity varies from V=0 m/s to V=3 m/s. However, above the tip of the convex blade, the velocity reaches its maximum value which is equal to V=13 m/s. In fact, it is related to the lift force created with the rotor rotation. Inside the rotation domain, the velocity slightly increases to the value of V=7 m/s. The area in the proximity of the convex blade manifests acceleration of velocity that reaches the value of V=13 m/s in the plane defined by x=0 mm. Here it is related to the flow passage from one blade to the other so that the turbine rotates. A

deceleration zone is observed downstream of the rotor and is deflected upward. As one gets farther away from the rotor, the velocity decreases and then gradually increases. Consequently, the wake phenomenon is presented.

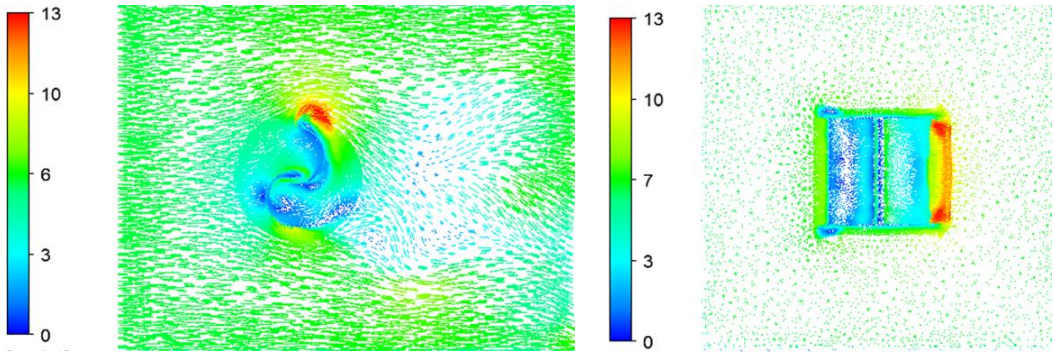

(a) (b)

Fig. 9. Velocity fields (m/s) (a) z=0 mm (b) x=0 mm

5.2 Total Pressure

Figure 10(a) and Figure 10(b) show the total pressure distribution in the longitudinal plane defined by z=0 mm as well as the transverse plane defined by x=0 mm. According to these results, the concave side of the advancing blade presents high pressure that reaches the value of p=20 Pa inside the blade and p=67 Pa above the tip of the blade, the gap between the two values is explained by the centrifuge force which higher on the tip of the blade. This pressure contributes in the creation of the positive torque. The convex side of the returning blade reveals a depression where the value of the pressure is equal to p=-39 Pa. This pressure contributes in the creation of the negative torque and so causes reduction of the net torque produced. Indeed, the convex side of the advancing blade manifests a depression where the value of the pressure is equal to p=-27 Pa. whereas, the concave side of the returning blade presents higher pressure that reaches the value of p=20 Pa. The pressure difference is responsible of the rotor rotation. A low pressure area is visible downstream. Because of the slow increase in velocity, it is related to the wake phenomena.

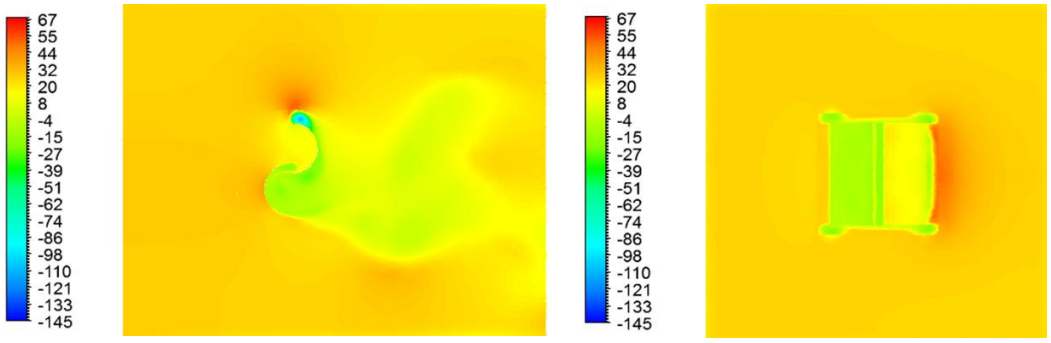

(a) (b)

Fig. 10. Total pressure distributions (Pa) (a) z=0 mm (b) x=0 mm

5.3 Turbulent Kinetic Energy

Figure 11(a) and Figure 11(b) show the distribution of the turbulent kinetic energy in the longitudinal plane defined by z=0 mm as well as the transverse plane defined by x=0 mm. From these results, the turbulent kinetic energy value is deniable downstream the rotor. The area

around the blades reveals an increase in its value and reaches k=2.056 J.kg^{-1}. It is noticeable that the zone upstream the rotor presents a remarkable increase in the value of the turbulent kinetic energy that is equal to k=3.084 J.kg^{-1}. This remarkable value is explained by the wind turbine extracting energy from downstream where wind speed is reduced. As the flow proceeds downstream, there is a spreading of the wake and the wake recovers towards free stream conditions. Indeed, it was observed that the turbulent kinetic energy is almost negligible in the test chamber. Whereas, near the turbine structure, it reaches the value of k=2.399 J.kg^{-1}, which is explained by the wake phenomenon mentioned previously.

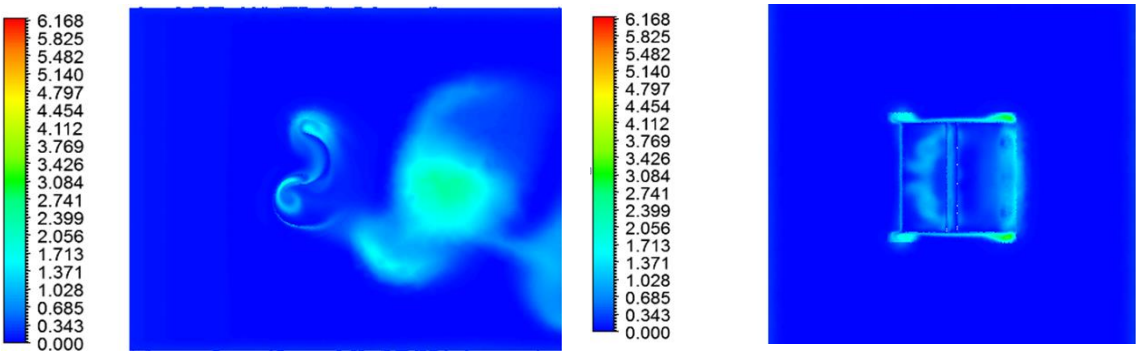

Fig. 11. Turbulent kinetic energy distribution (J.kg^{-1}) (a) z=0 mm (b) x=0 mm

5.4 Turbulent Viscosity

Figure 12(a) and Figure 12(b) show the distribution of the turbulent viscosity in the longitudinal plane defined by z=0 mm as well as the transverse plane defined by x=0 mm. From these results, the turbulent viscosity is negligible in the test chamber and its value is almost null. However, the concave sides of the blades reveal higher values where the turbulent viscosity is equal to μ_t=130 Pa.s Upstream the rotor, it peaks to reach μ_t=470 Pa.s which is explained by the wake phenomena mentioned previously. As for the transverse plane, the value of the turbulent viscosity remains null for almost the entire test section except near the rotor walls where it slightly increases. There are more eddies in the flow the more turbulent it is. Actually, one may think of the turbulent flow as an erratic eddy. Because of the fluctuations, the air velocity at every point in the computational domain is constantly changing in both direction and magnitude. There is a flow wake creation as one moves away from the rotor.

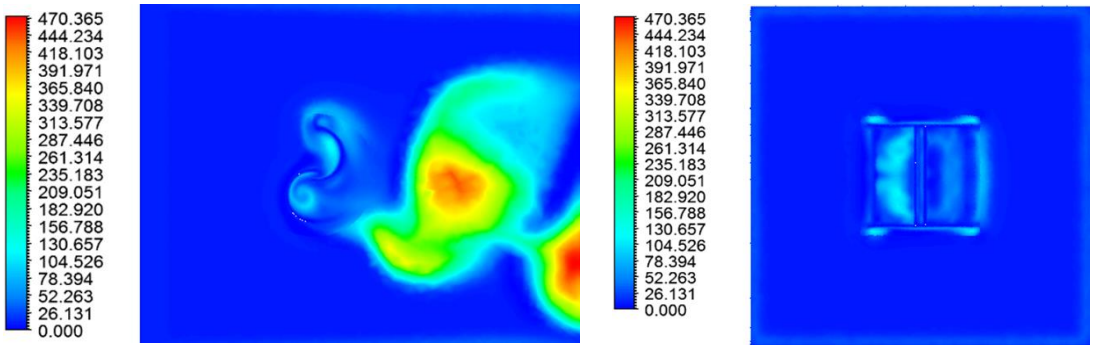

Fig. 12. Turbulent viscosity distribution (Pa.s) (a) z=0 mm (b) x=0 mm

6. Conclusions

In this paper, three dimensional transient simulations were carried out with the use of the CFD code Ansys Fluent to show the effect of the numerical model parameters choice on a Savonius wind rotor performances. The effect of the mesh sizing, the turbulence model as well as the time step were investigated. The numerical model validation was performed based on earlier experimental findings found in the literature for an inlet velocity of $6ms^{-1}$. In terms of mesh selection, the one that was selected was picked since it had a significant number of nodes with good accuracy and time savings. The SST k-ω was chosen for the turbulence model based on its good agreement with the experimental data and its prior works as reported in the literature. For the time step, it was picked as, in comparison to the experimental findings, it produced good agreement and enhanced the numerical results. Under these conditions, the numerical model with the selected parameters was found in agreement with the experimental findings provided in the literature with an average error equal to 8.8%. For a tip speed ratio λ=0.64 it gave a torque and power coefficients equal to 0.328 and 0.2, respectively.

Acknowledgements

This work was supported by the sustainable Mobility Center (Centro Nazionale per la Mobilita Sostenibile –CNMS) under Grant CN000000023 CUP B73C22000760001.

References

[1] Kamaruddin, Noorfazreena, and Muhd Syukri Mohd Shamsuddin. "Experimental Investigation of the Power Storage System for Savonius Turbines in Wind and Water." *Journal of Advanced Research in Applied Sciences and Engineering Technology* 28, no. 3 (2022): 235-247.

[2] Roslan, Siti Amni Husna, Zainudin A. Rasid, and Ahmad Kamal Ariffin. "Extended blade element momentum theory for the design of small-scale wind turbines." *Journal of Advanced Research in Applied Mechanics* 101, no. 1 (2023): 62-75. https://doi.org/10.37934/aram.101.1.6275

[3] Alotaibi, Alowaid, Mohd Khairul Hafiz Muda, Faizal Mustapha, Izhal Abdul Halin, and Noorfaizal Yidris. "Perpetual Motion Wind Turbine Generator for Novelty Energy Harvesting System; Conceptual Design Approach." *Journal of Advanced Research in Fluid Mechanics and Thermal Sciences* 94, no. 2 (2022): 166-173. https://doi.org/10.37934/arfmts.94.2.166173.

[4] Kamdar, Ismail, and Juntakan Taweekun. "A Comparative Study of Wind Characteristics Between South-Western and South-Eastern Thailand Using Different Wind Turbine Models." *Journal of Advanced Research in Fluid Mechanics and Thermal Sciences* 92, no. 1 (2022): 149-161. https://doi.org/10.37934/arfmts.92.1.149161.

[5] Asadbeigi, Mohammadreza, Farzad Ghafoorian, Mehdi Mehrpooya, Sahel Chegini, and Azad Jarrahian. "A 3D study of the darrieus wind turbine with auxiliary blades and economic analysis based on an optimal design from a parametric investigation." *Sustainability* 15, no. 5 (2023): 4684. https://doi.org/10.3390/su15054684

[6] Ebrahimpour, Mohammad, Rouzbeh Shafaghat, Rezvan Alamian, and Mostafa Safdari Shadloo. "Numerical investigation of the Savonius vertical axis wind turbine and evaluation of the effect of the overlap parameter in both horizontal and vertical directions on its performance." *Symmetry* 11, no. 6 (2019): 821. https://doi.org/10.3390/sym11060821

[7] Sobczak, Krzysztof. "Numerical investigations of an influence of the aspect ratio on the Savonius rotor performance." In *Journal of Physics: Conference Series*, vol. 1101, no. 1, p. 012034. IOP Publishing, 2018. https://doi.org/10.1088/1742-6596/1101/1/012034

[8] Lee, Jae-Hoon, Young-Tae Lee, and Hee-Chang Lim. "Effect of twist angle on the performance of Savonius wind turbine." *Renewable Energy* 89 (2016): 231-244. https://doi.org/10.1016/j.renene.2015.12.012

[9] Tahani, Mojtaba, Ali Rabbani, Alibakhsh Kasaeian, Mehdi Mehrpooya, and Mojtaba Mirhosseini. "Design and numerical investigation of Savonius wind turbine with discharge flow directing capability." *Energy* 130 (2017): 327-338. https://doi.org/10.1016/j.energy.2017.04.125.

[10] Tian, Wenlong, Zhaoyong Mao, Baoshou Zhang, and Yanjun Li. "Shape optimization of a Savonius wind rotor with different convex and concave sides." *Renewable energy* 117 (2018): 287-299. https://doi.org/10.1016/j.renene.2017.10.067

[11] Nurmutia, Syahreen, Bukhari Manshoor, Amir Khalid, Izzuddin Zaman, Djamal Hissein Didane, Reazul Haq Abdul Haq, Mohammad Fahmi Abdul Ghafir *et al.,* "Performance Analysis on a New Design of Blade Shape for Savonius Wind Turbine." *Journal of Advanced Research in Fluid Mechanics and Thermal Sciences* 108, no. 1 (2023): 173-183. https://doi.org/10.37934/arfmts.108.1.173183.

[12] Akhlaghi, M., and F. Ghafoorian. "Investigation of arc angle rotor blade variations effect of Savonius vertical axis wind turbine on power and torque coefficients using a 3D modeling." *Renewable Energy Research and Applications* 4, no. 1 (2023): 13-19. https://doi.org/10.22044/rera.2022.11282.1084

[13] Abdelsattar, Sohib, Nurul Asyikin Abu Bakar, and Noorfazreena Mohammad Kamaruddin. "Performance of Savonius Turbines with Tubercles Inspired by Humpback Whales." *Journal of Advanced Research in Applied Sciences and Engineering Technology* 31, no. 1 (2023): 68-78. https://doi.org/10.37934/araset.31.1.6878.

[14] Jeon, Keum Soo, Jun Ik Jeong, Jae-Kyung Pan, and Ki-Wahn Ryu. "Effects of end plates with various shapes and sizes on helical Savonius wind turbines." *Renewable energy* 79 (2015): 167-176. https://doi.org/10.1016/j.renene.2014.11.035

[15] Zheng, M., X. Zhang, L. Zhang, H. Teng, J. Hu, and M. Hu. "Uniform test method optimum design for drag-type modified Savonius VAWTs by CFD numerical simulation." *Arabian Journal for Science and Engineering* 43 (2018): 4453-4461. https://doi.org/10.1007/s13369-017-2920-5

[16] Emmanuel, Binyet, and Wang Jun. "Numerical study of a six-bladed Savonius wind turbine." (2011): 044503. https://doi.org/10.1115/1.4004549

[17] Mohamed, M. H., G. Janiga, E. Pap, and D. Thévenin. "Optimization of Savonius turbines using an obstacle shielding the returning blade." *Renewable Energy* 35, no. 11 (2010): 2618-2626. https://doi.org/10.1016/j.renene.2010.04.007

[18] Payambarpour, S. Abdolkarim, Amir F. Najafi, and Franco Magagnato. "Investigation of deflector geometry and turbine aspect ratio effect on 3D modified in-pipe hydro Savonius turbine: Parametric study." *Renewable Energy* 148 (2020): 44-59. https://doi.org/10.1016/j.renene.2019.12.002

[19] Farajyar, Shayan, Farzad Ghafoorian, Mehdi Mehrpooya, and Mohammadreza Asadbeigi. "CFD investigation and optimization on the aerodynamic performance of a Savonius vertical axis wind turbine and its installation in a hybrid power supply system: a case study in Iran." *Sustainability* 15, no. 6 (2023): 5318. https://doi.org/10.3390/su15065318

[20] Roy, Sukanta, and Ujjwal K. Saha. "Wind tunnel experiments of a newly developed two-bladed Savonius-style wind turbine." *Applied Energy* 137 (2015): 117-125. https://doi.org.10.1016/j.apenergy.2014.10.022

[21] Tey, Wah Yen, and Hooi Siang Kang. "Power Loss in Straight Polygon Pipe via CFD Simulation." *Progress in Energy and Environment* (2018): 1-10.

[22] Nazer, Mohamed, Muhammad Fadzrul Hafidz Rostam, Se Yong Eh Noum, Mohammad Taghi Hajibeigy, Kamyar Shameli, and Ali Tahaei. "Performance analysis of photovoltaic passive heat storage system with microencapsulated paraffin wax for thermoelectric generation." *Journal of Research in Nanoscience and Nanotechnology* 1, no. 1 (2021): 75-90. https://doi.org/10.37934/jrnn.1.1.7590.

[23] Shaharudin, Muhammad Zarif Bin, Syahar Shawal, Mazwan Mahat, and Mohd Rosdzimin Abdul Rahman. "Numerical Investigation on Thermal Performance of Various Designs Plate-Fin Heat Sinks Subject to Parallel and Impinging Flow." *Journal of Advanced Research in Numerical Heat Transfer* 13, no. 1 (2023): 66-80. https://doi.org/10.37934/arnht.13.1.6680

[24] Elfaghi, Abdulhafid MA, Alhadi A. Abosbaia, Munir FA Alkbir, and Abdoulhdi AB Omran. "CFD Simulation of Forced Convection Heat Transfer Enhancement in Pipe Using Al2O3/Water Nanofluid." *Journal of Advanced Research in Micro and Nano Engineering* 7, no. 1 (2022): 8-13.

[25] Islam, Md Saifi Bin, Muhammad Faiz Ahmed, and Abdullah Al Saad. "Numerical Investigation on the Aerodynamic Characteristics of a Wing for Various Flow and Geometrical Parameters." *Malaysian Journal on Composites Science and Manufacturing* 12, no. 1 (2023): 13-30. https://doi.org/10.37934/mjcsm.12.1.1330

[26] Mehrpooya, Mehdi, Mohammadreza Asadbeigi, Farzad Ghafoorian, and Shayan Farajyar. "Investigation and optimization on effective parameters of a H-rotor Darrieus wind turbine, using CFD method." *Iran. J. Chem. Chem. Eng* (2023). https://doi./org.10.30492/ijcce.2023.562396.5610

[27] Akhlaghi, M., M. Asadbeigi, and F. Ghafoorian. "Novel CFD and DMST dual method parametric study and optimization of a Darrieus vertical axis wind turbine." *Journal of Applied Fluid Mechanics* 17, no. 1 (2023): 205-218. https://doi.org/10.47176/jafm.17.1.1985

[28] Akhlagi, Mohammad, Farzad Ghafoorian, Mehdi Mehrpooya, and Mohsen Sharifi Rizi. "Effective parameters optimization of a small scale Gorlov wind turbine, using CFD method." *Iran. J. Chem. Chem. Eng. Research Article Vol* 42, no. 7 (2023). https://doi.org/10.30492/ijcce.2022.561960.5584.

[29] Ghafoorian, Farzad, Seyed Reza Mirmotahari, Farnaz Bakhtiari, and Mehdi Mehrpooya. "Exploring optimal configurations for a wind farm with clusters of Darrieus VAWT, using CFD methodology." *Journal of*

Computational Applied Mechanics 54, no. 4 (2023): 533-551. https://doi.org/10.22059/jcamech.2023.363102.857.

[30] Chegini, Sahel, Mohammadreza Asadbeigi, Farzad Ghafoorian, and Mehdi Mehrpooya. "An investigation into the self-starting of Darrieus-Savonius hybrid wind turbine and performance enhancement through innovative deflectors: A CFD approach." *Ocean Engineering* 287 (2023): 115910. https://doi.org/10.1016/j.oceaneng.2023.115910.

[31] Abid, Hasna, Ahmed Ketata, Mariem Lajnef, Hamza Chiboub, and Zied Driss. "Numerical investigation of greenhouse climate considering external environmental factors and crop position in Sfax central region of Tunisia." *Solar Energy* 264 (2023): 112032. https://doi.org/10.1016/j.solener.2023.112032.

[32] Mosbahi, Mabrouk, Mouna Derbel, Mariem Lajnef, Bouzid Mosbahi, Zied Driss, Costanza Aricò, and Tullio Tucciarelli. "Performance study of twisted Darrieus hydrokinetic turbine with novel blade design." *Journal of Energy Resources Technology* 143, no. 9 (2021): 091302. https://doi.org/10.1115/1.4051483

[33] Mosbahi, Mabrouk, Mariem Lajnef, Mouna Derbel, Zied Driss, Emanuele Amato, Calogero Picone, Marco Sinagra, and Tullio Tucciarelli. "Effect of the Turbulence Model on the Computational Results of a Lucid Spherical Rotor." *Journal of Advanced Research in Fluid Mechanics and Thermal Sciences* 113, no. 1 (2024): 24-43. https://doi.org/10.37934/arfmts.113.1.2443.

[34] Mosbahi, Mabrouk, Mariem Lajnef, Mouna Derbel, Bouzid Mosbahi, Costanza Aricò, Marco Sinagra, and Zied Driss. "Performance improvement of a drag hydrokinetic turbine." *Water* 13, no. 3 (2021): 273. https://doi.org/10.3390/w13030273

[35] Lajnef, Mariem, Mabrouk Mosbahi, Youssef Chouaibi, and Zied Driss. "Performance improvement in a helical Savonius wind rotor." *Arabian Journal for Science and Engineering* 45, no. 11 (2020): 9305-9323. https://doi.org/10.1007/s13369-020-04770-6